

Highly Sustained Release of Bactericides from Complex Coacervates

Sabrina S. Alam,¹ Youngwoo Seo^{1,2,*} and Yakov Lapitsky^{1,*}

¹ Department of Chemical Engineering, University of Toledo, Toledo, Ohio 43606

² Department of Civil and Environmental Engineering, University of Toledo, Toledo, Ohio 43606

* Corresponding authors: yakov.lapitsky@utoledo.edu
youngwoo.seo@utoledo.edu

ABSTRACT: Materials for preventing harmful bacterial contamination attract widespread interest in areas that include healthcare, home/personal care products, and crop protection. One approach to achieving this functionality is through the sustained release of antibacterial compounds. To this end, we show how putty-like complex coacervates, formed through the association of poly(allylamine hydrochloride) (PAH) with pentavalent tripolyphosphate (TPP) ions, can provide a sustained antibacterial effect by slowly releasing bactericides. Using triclosan (TC) as a model bactericide, we demonstrate that, through their dispersion in the parent PAH solution with nonionic surfactants, hydrophobic biocides can be efficiently and predictably encapsulated within PAH/TPP coacervates. Once encapsulated, the bactericide can be released over multiple months, and the release rates can be readily tuned by varying the bactericide and surfactant compositions used during encapsulation. Through this release, the PAH/TPP coacervates provide sustained bactericidal activity against model gram-positive and gram-negative bacteria (*Staphylococcus aureus* and *Escherichia coli*) grown under a nutrient-rich condition over at least two weeks. Thereafter, though some partial activity persists after one month, the release slows down and the bactericide-eluting coacervates lose their efficacy. Overall, we show that bactericide release from easy-to-prepare complex coacervates can provide a pathway to sustained disinfection.

Keywords: Long-Term Release, Coacervates, Ionic Networks, Disinfection, Antimicrobial Activity

1. INTRODUCTION

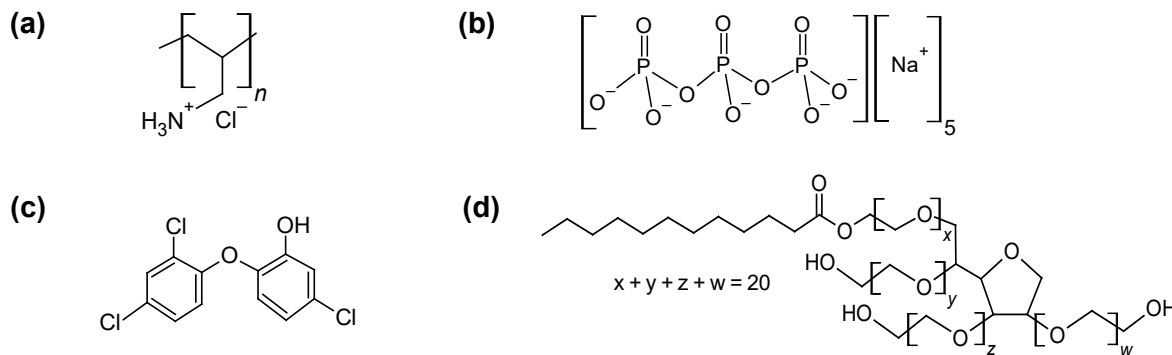
Bacterial contamination causes numerous costly problems, including human diseases and mortality,^{1, 2} food and consumer product spoilage,^{3, 4} crop diseases,^{5, 6} biofouling,⁷ and pipe/equipment corrosion.^{8, 9} To address these challenges, bactericides (i.e., disinfectants, antiseptics and antibiotics) are widely used in healthcare, professional cleaning, water purification, food processing, coatings, and consumer product formulations.^{10, 11} Despite their broad utility, however, use of these active molecules frequently presents problems such as their toxicity,¹² need for repeated application, and limited chemical stability.¹³ To this end, there has been substantial interest in the controlled release of disinfectants for long-term prevention of bacterial growth.¹³⁻¹⁷ This approach mitigates the need for repeated application, (through encapsulation) protects the active compounds from degrading¹³ and, by moderating the amounts in which these antibacterial payloads are released, reduces the toxicity associated with their application.^{12, 18}

The controlled bactericide release systems developed to date include plastic films,^{16, 17, 19} wafers,^{20, 21} beads,¹⁹ and a diverse array of micro- and nanoparticles,^{18, 22, 23} fibers,^{24, 25} coatings^{15,}^{26, 27} and gels,²⁸⁻³¹ all of which have been used for encapsulating and slowly releasing biocidal small molecules. Among these sustained release vehicles are materials prepared through polyelectrolyte self-assembly.^{15, 32-34} These biocide-eluting materials have been prepared through two general approaches: (1) preparation of polyelectrolyte complex multilayers (PEMs), where tens of alternating layers of anionic and cationic polyelectrolyte layers were deposited on surfaces;^{15, 32-34} and (2) complex coacervation, where complexes between a polyelectrolyte and an oppositely charged polymer,^{35, 36} protein^{22, 37} or multivalent ions^{38, 39} were formed by simply mixing the two associating solutes in aqueous solution. In recent years, PEMs have been shown to provide antibacterial and antifungal activity over multi-week and multi-month timescales.^{40, 41} To

our knowledge, however, despite their much simpler preparation, such long-term antibacterial activity has not been demonstrated for complex coacervates.

Recently, one of us hypothesized that highly sustained disinfection could be achieved using putty-like complex coacervates formed from aqueous mixtures of the cationic polymer, poly(allylamine hydrochloride) (PAH) and pentavalent anion, tripolyphosphate (TPP) (see Scheme 1a and b).⁴² These coacervates can both adhere to diverse surfaces^{43, 44} and release small molecules over multiple months.^{42, 45} The long-term sustained release functionality of PAH/TPP coacervates likely reflects their high network densities and has, to date, been demonstrated using water-soluble (anionic and zwitterionic) dyes⁴² and the anti-inflammatory drug, ibuprofen.⁴⁵ Besides their adhesion and long-term release functionalities, PAH/TPP coacervates have shown promising cytocompatibilities with human cells, which suggests these materials to be relatively nontoxic.⁴² Indeed, PAH (in its covalently crosslinked form) is already used as an oral drug,⁴⁶ and TPP is on the U.S. Food and Drug Administration's generally regarded as safe (GRAS) list. These favorable properties, along with the ability of PAH/TPP coacervates to adhere to a surface and release small molecules over extended timescales, suggest these multifunctional self-assembled materials as attractive long-term sustained release vehicles for a broad range of potential applications.

Scheme 1. Molecular structures of (a) PAH, (b) TPP, (c) TC and (d) TW.



Building on these findings, here we investigate the use of PAH/TPP coacervates for the highly sustained release of antibacterial agents, with the view of developing products for sustained household, institutional, and (eventually) medical disinfection — e.g., where the bactericide-eluting PAH/TPP coacervates are attached to (or incorporated within) wet surfaces or devices, ranging from the insides of showerheads to infection-prone surgical implants. Further, by using a hydrophobic, sparingly soluble molecule, Triclosan (TC; Scheme 1c)^{47,48} as the model bactericide we, for the first time, characterize the multifunctional PAH/TPP coacervates as materials for the long-term release of hydrophobic payloads, which — despite being often encapsulated in biopolymeric (e.g., gelatin/anionic polysaccharide) coacervates^{22, 35-37, 49, 50} — have not yet been used with the PAH/TPP system.

To perform this study, TC encapsulation effects on PAH/TPP coacervation were first examined, after which the TC uptake performance of the resulting PAH/TPP coacervates was quantified. To target applications in household and institutional disinfection, tap water (such as might be found in bathrooms, kitchens or dental unit waterlines) was used as the release medium, wherein coacervate swelling and TC release were measured. Finally, the antibacterial efficacy of the TC-eluting PAH/TPP coacervates against planktonic bacteria was examined over roughly 2 months using *Staphylococcus aureus* (*S. aureus*) and *Escherichia coli* (*E. coli*) as model gram-positive and gram-negative bacterial strains, respectively.

2. MATERIALS AND METHODS

2.1. Materials

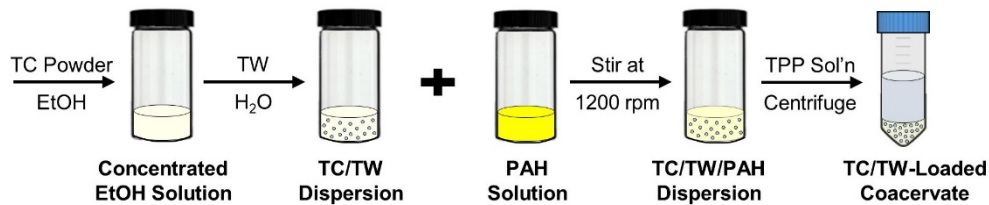
Deionized water (18.2 MΩ·cm resistivity) was obtained from a Millipore Direct-Q water purification system. PAH (nominal molecular weight \approx 150 kDa; 40 wt% solution) was purchased

from Nittobo Co. (Tokyo, Japan). TC, TPP (sodium salt), thiazole orange, and ninhydrin reagent (2,2-dihydroxyindane-1,3-dione) were obtained from Sigma-Aldrich (St. Louis, MO). Tween 20 (TW) surfactant (Scheme 1d), propidium iodide, paraformaldehyde, ethanol (EtOH), dimethyl sulfoxide (DMSO) and hydrochloric acid (HCl) were purchased from Fisher Scientific (Fair Lawn, NJ), while sodium hydroxide (NaOH) was supplied by VWR (West Chester, PA). All materials were used as received.

2.2 Preparation of TC-Loaded Coacervates

TC-loaded PAH/TPP coacervates were prepared as shown in Scheme 2. To disperse the TC in water, it was first dissolved in 86 wt% EtOH, and then mixed with aqueous TW solutions in 0.25 – 1.00:1 TW:TC molar ratios (and a constant 0.22:1 TC:EtOH molar ratio). The mixtures were then stirred at 400 rpm overnight with 12 mm × 4 mm cylindrical magnetic stir bars. The resulting TC/TW/EtOH/water mixtures were then mixed with 20 wt% (2.4 M in their monomer concentrations) PAH solutions in a 1:1 volumetric ratio (and stirred at 1200 rpm for overnight) to prepare TC-charged 10 wt% (1.2 M) PAH mixtures (Scheme 2). To generate TC-loaded PAH/TPP coacervates, 0.8 mL of 7.5 wt% (220 mM) TPP solution and 0.75 mL of PAH/TC mixture were added to 1.5 mL microcentrifuge tubes and vortexed for 5 – 10 s. The tubes were then centrifuged at 15000 rpm for 90 min, whereupon the coacervates were separated from the supernatant phases for analysis. Similarly, control coacervates (without any TC, TW or EtOH and with TW/EtOH only) were prepared via the same method.

Scheme 2. Preparation of the TC/TW-loaded PAH/TPP coacervates.



2.3. Analysis of PAH/TPP Complexation

The PAH/TPP association within the coacervates could be affected by their composition (e.g., their pH/ionic strength⁴⁴ or payload content⁴⁵). Thus, the PAH/TPP complexation efficiency was examined by quantifying the free PAH concentrations within the supernatant and coacervate phases. The supernatant PAH concentration was used to estimate the fractions of PAH chains that, through PAH/TPP complexation, ended up in the coacervate (i.e., the yield of the coacervation process). To quantify free PAH in the supernatant, 0.5 mL of supernatant solution was added to a 6 mL glass test tube, whereupon 0.5 mL of ninhydrin reagent was added to each tube. The tubes were then capped, shaken and heated in a boiling water bath for 30 min. They were then cooled in a 25 °C water bath for 10 min, after which 2.5 mL of 50 vol% water/EtOH mixture was added to each tube, and the tubes were vortexed for 30 s. The PAH content was then determined via absorbance measurements (at $\lambda = 570$ nm) with a Cary 50 UV-vis spectrometer (Sparta, NJ), which revealed the PAH yield as:

$$\%Yield = \left(\frac{C_i - C_s}{C_i} \right) \times 100\% \quad (1)$$

where C_i was the initial (i.e., overall) PAH concentration obtained upon mixing of PAH with TPP, and C_s was the free PAH concentration remaining in the supernatant. Further insight into the TC uptake effect on the PAH/TPP complexation was obtained by estimating its impact on the PAH concentration within the coacervate. This analysis was performed by weighing the coacervate

phases and dividing the PAH weights they contained (obtained via the ninhydrin assay) by their total weights. Each coacervate type was analyzed using three replicate samples.

2.4. TC Uptake Analysis

To measure TC encapsulation efficiency, the supernatant phases were carefully collected for further analysis, right before the freshly formed coacervates were centrifuged into pellets. This step was crucial to avoid sedimenting the TC/TW dispersions in the supernatant phase onto the coacervate surface. The supernatant TC concentration was then determined via UV-vis spectroscopy, which required the sparingly soluble TC to first be fully dissolved. To dissolve the colloidally dispersed TC, the supernatant phases were diluted in 20 wt% EtOH aqueous solutions that contained 10 mM NaOH, whereupon the supernatant TC concentrations were quantified through UV-vis absorbance readings at $\lambda = 292$ nm ($\varepsilon = 40 \text{ mM}^{-1} \text{ cm}^{-1}$). These concentrations were then used to determine the TC loading capacity (*LC*) and loading efficiency (*LE*) as:

$$LC = \left(\frac{V_t C_i - V_s C_s}{W_0} \right) \times 100\% \quad (2)$$

$$LE = \left(\frac{V_t C_i - V_s C_s}{V_t C_i} \right) \times 100\% \quad (3)$$

where C_i is the initial overall TC concentration in the parent PAH/TPP/TC/TW mixture added to the microcentrifuge tube, C_s is the final TC concentration remaining in the supernatant, V_t is the total mixture volume added to the microcentrifuge tube, V_s is the supernatant volume recovered after centrifugation, and W_0 is the coacervate weight (also measured after centrifugation). Besides varying the TC concentrations (as described in Section 2.2), the *LC* and *LE* values of the TC/TW-

loaded coacervates were measured at variable TW:TC molar ratios (at a constant TPP:PAH molar ratio of 0.2:1). Each uptake experiment was repeated thrice to ensure reproducibility.

2.5. Gravimetric Analysis of Coacervate Swelling

The stability of TC-loaded PAH/TPP coacervates in tap water ($\text{pH} \approx 9.6 \pm 0.4$) was probed by gravimetry. The initial coacervate weight was measured after removing the supernatant from the microcentrifuge tube and then gently wiping the coacervate surface with a KimwipeTM tissue. The coacervates were then equilibrated in an Eppendorf Thermomixer (Hamburg, Germany) at 400 rpm in 1 mL of dechlorinated tap water at 25 °C (with the water replaced daily) and weighed every 4 d to determine changes in their weights. Their weights were then normalized to the initial values as $W(t)/W_0$, where $W(t)$ was the weight at time, t , and W_0 was the weight prior to tap water immersion. Similar measurements were taken for control coacervates prepared without any TC or TW, with each sample type analyzed in triplicate.

2.6. TC Release Rate Analyses

TC release into the dechlorinated tap water was then analyzed via UV-vis spectroscopy, by measuring absorbance at $\lambda = 292 \text{ nm}$ ($\varepsilon = 40 \text{ mM}^{-1} \text{ cm}^{-1}$). To eliminate turbidity artifacts, all release media samples were diluted in 20 wt% EtOH and 10 mM NaOH aqueous solution (to fully solubilize any undissolved TC) before their analysis. To begin this experiment, 1 mL of tap water (described in Section 2.5) was poured over the coacervate pellets at the bottoms of the microcentrifuge tubes. The tap water was then replaced daily with the release from each coacervate sample measured after each solvent replacement step.

Additionally, since TC is only sparingly soluble (which could make maintaining sink conditions during the release experiments challenging),⁵¹ further release experiments were performed to assess the impact of the release medium volume on its release rates. Here, the 2 mL flat-capped microcentrifuge tubes ($\varnothing = 11$ mm) containing the coacervate pellets were stripped of their caps and fitted inside 15 mL FalconTM centrifuge tubes ($\varnothing = 17$ mm). The larger tubes were then filled with 10 mL of tap water, which increased the release medium volume tenfold, and agitated at 600 rpm and 25 °C on a Multi-ThermTM shaker (Benchmark Scientific; South Plainfield, NJ). The tap water was, again, periodically replaced and analyzed via UV-vis spectroscopy for the released TC; daily at first, and then, once TC release slowed down, every 2 d. Each release experiment was repeated thrice to ensure reproducibility.

2.7. Antimicrobial Activity Analysis

To probe the effectiveness of bactericide-eluting PAH/TPP coacervates in long-term disinfection, two model bacteria were used: gram-positive *S. aureus* (ATCC 25923) and gram-negative *E. coli* (ATCC 25922). Long-term release of TC into fresh bacterial culture (which was replenished daily) was performed over 2 months. Coacervate pellets (0.15 – 0.22 g) each prepared in 1.5 mL microcentrifuge tubes (with caps removed) were fitted inside 15 mL FalconTM centrifuge tubes. Ten mL aliquots of freshly cultured bacterial suspensions in one-tenth strength Luria-Bertani (LB) broth (OD = 0.1 ± 0.01; corresponding cell number ~10⁷ cfu/mL) were then added on top of the coacervates inside the 15 mL centrifuge tubes, whereupon the tubes were incubated at 200 rpm and 37 ± 1 °C for 24 ± 4 h. To convincingly show that the bactericidal activity is mediated by the long-term sustained release (and not by the bactericide in the release media released earlier in the experiment), the bacterial suspensions were then replaced daily with freshly cultured suspensions

in TC-free media. Bacterial growth was monitored based on changes in OD, which were recorded every 2 d. Bacterial cell viability was also analyzed using an upright fluorescence microscope (Olympus BX-51; Tokyo, Japan). Here, to distinguish live and dead cells, 5 μ L of 42 μ M thiazole orange in DMSO and 5 μ L of 4.3 mM aqueous propidium iodide solution were added to 500 μ L cell dispersion aliquots to stain the cells.

Prior to imaging, the cells were fixed using a 4 vol% paraformaldehyde solution at room temperature. To concentrate the cells, their dispersions were first separated from the coacervates and centrifuged in the 15 mL FalconTM tubes for 20 min at 5000 rpm (4300 g), after which 5 mL of the cell-rich dispersions from the tube bottoms were collected for the analysis. All images were captured using a 100 \times objective and slides equipped with 1 mm² grids and analyzed using ImageJ software (National Institutes of Health; Bethesda, MD). This experiment was continued until all observable antibacterial activity of TC-loaded coacervates was lost. Moreover, to ascertain the effect of the eluted TC on the bacteria, bacterial growth was monitored under three control conditions: (1) without coacervate, (2) with an empty coacervate, and (3) with a TW-loaded (but TC-free) coacervate. To ensure reproducibility, three replicate samples ($n = 3$) were used at each experimental condition and 6 images were captured from each slide. Statistical differences ($p < 0.05$) between the viability of coacervate-free cells and cells exposed to the coacervates (both with and without TC) were then assessed via the one-way analysis of variance (ANOVA) followed by a Dunnett's *post hoc* test.

3. RESULTS AND DISCUSSION

3.1. Coacervate Formation

Coacervates formed immediately upon the mixing of PAH with the TPP and adhered to the microcentrifuge tubes. The coacervates loaded with TW and TC/TW mixtures, however, were whiter/opaquer (Figure 1a) and less adhesive — i.e., unlike their empty counterparts, they detached from the tube walls when vigorously shaken. Additionally, although both TC and TW were nonionic (and were thus not expected to competitively associate with PAH or TPP⁴⁵), the TC/TW dispersions in the parent PAH solutions appeared to interfere with PAH/TPP complexation. As the TC concentration was raised from 0 to 160 mM, the PAH yield within the coacervate phases dropped by up to 5% (see Figure 1b). This effect was greatest at the highest TC concentrations and TW:TC ratios, and suggested the possibility of the payload sterically hindering the PAH/TPP association. Nonetheless, the average PAH yield remained above 90% at every tested composition, indicating these inhibitive effects to be relatively minor.

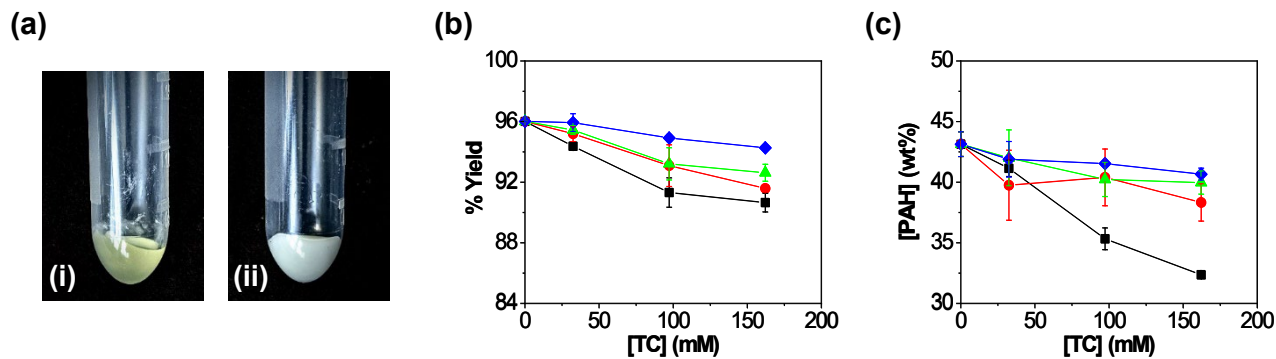


Figure 1. Effect of TC encapsulation on the (a) visual appearance of (i) empty and (ii) TC/TW-loaded coacervates, (b) PAH yield and (c) PAH concentration within the coacervate when the TC is dispersed in the parent PAH solutions using (◆) 0.25:1, (▲) 0.33:1, (●) 0.50:1 and (■) 1.00:1 TW:TC molar ratios. All data are mean \pm SD, while the lines are guides to the eye.

Interestingly, besides slightly reducing PAH/TPP complexation, the TC uptake decreased the PAH concentration within the coacervates (Figure 1c). The extent of this decrease depended

strongly on the TW:TC molar ratio. At the lowest, 0.25:1 TW:TC molar ratio, the reduction in the average PAH concentration within the coacervate (as the TC concentration added to the parent PAH solution was raised from 0 to 160 mM) was very small (from 43 to 41 wt%). As the TW:TC molar ratio was raised to 1:1, however, the PAH concentration within the coacervate dropped significantly, from 43 to 32 wt%. This drop in the PAH concentration suggested that the PAH/TPP ionic networks became more porous; presumably, due to a high colloid concentration within the network. Since the TW molecular weight (1228 g/mol) was more than four times greater than that of TC (289.5 g/mol), the dispersion of 160 mM (47 mg/mL) TC at a 1:1 TW:TC molar ratio corresponded to 23 wt% of combined TC/TW concentration in the 10 wt% parent PAH solution. Because most of this solute existed in either particulate or micellar form, its presence expectedly increased the porosity of the PAH/TPP network and so decreased its overall PAH concentration. Thus, though the TC/TW uptake had little effect on the PAH yield, its impact on the network structure may have been more significant.

3.2. TC Encapsulation Efficiency

The TC content within the PAH/TPP coacervates scaled linearly with the initial TC concentration in the parent PAH solution (Figure 2a). The slope of this line, however, depended on the TW:TC ratio and decreased by nearly 40% as the TW:TC molar ratio increased from 0.25 to 1.00:1. This variation in slope reflected variability in the LE. At the lowest TW:TC ratio, the LE — which remained insensitive to the TC concentration — was at nearly 100% (Figure 2b). As the surfactant content increased, however, the LE dropped to roughly 60%. This drop in LE coincided with the supernatant phase obtained upon PAH/TPP complexation becoming more turbid (Supporting Information, Figure S1), thus indicating that the dispersed TC particles were

less-efficiently encapsulated during the coacervation process. This effect may have reflected the high TW contents in the parent PAH solution during coacervation at the higher TW:TC ratios, which may have both enhanced the solubilization of the TC into the supernatant phase and (by sterically inhibiting the formation of the PAH/TPP networks) allowed for the TW-coated TC particles to be released from the coacervate before the polymer-rich PAH/TPP matrix could fully form. Regardless of the reasons for these differences in LE, however, very high TC loadings, exceeding 200 mg/g (or 20 wt% TC; see Figure 2a) were achieved and were easily and predictably controlled. Moreover, this encapsulation procedure was highly efficient, with most of the LE-values exceeding 80% (Figure 2b). These findings suggest that, similar to previous reports on hydrophobic molecule encapsulation using complex coacervates,^{37, 49, 50} PAH/TPP complexes are highly efficient in encapsulating hydrophobic payloads.

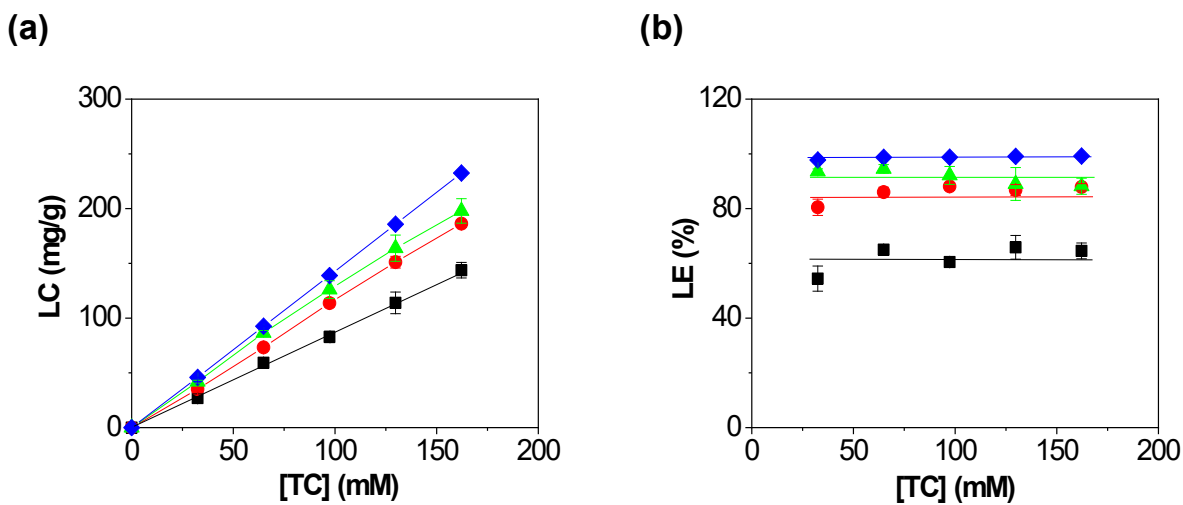


Figure 2. Effect of the initial TC concentration in the parent PAH solution on its (a) LC and (b) LE within the PAH/TPP coacervates obtained using (◆) 0.25:1, (▲) 0.33:1, (●) 0.50:1 and (■) 1.00:1 TW:TC molar ratios during encapsulation. All data are mean \pm SD, while the lines are guides to the eye.

3.3. Swelling of TC-Loaded Coacervates

While the empty control coacervates swelled by only 30% in tap water during the long-term release experiment, all TC/TW-loaded coacervates swelled to roughly 2 – 4 times their initial weight (Figure 3). This swelling increased with the TC loading and (especially at the higher TC loading) with the TW:TC ratio. In each case, the payload-induced swelling gradually increased over the first two weeks, and then remained roughly constant. The impacts of TC and TW addition on this swelling likely reflected the TC/TW effects on PAH/TPP association. As these additives were introduced, they hindered PAH/TPP association and generated TC/TW-filled pores in the coacervate networks. The less-complete PAH/TPP association, in turn — along with the increased solute/pore contents within the coacervate networks, likely increased the osmotic coacervate swelling.

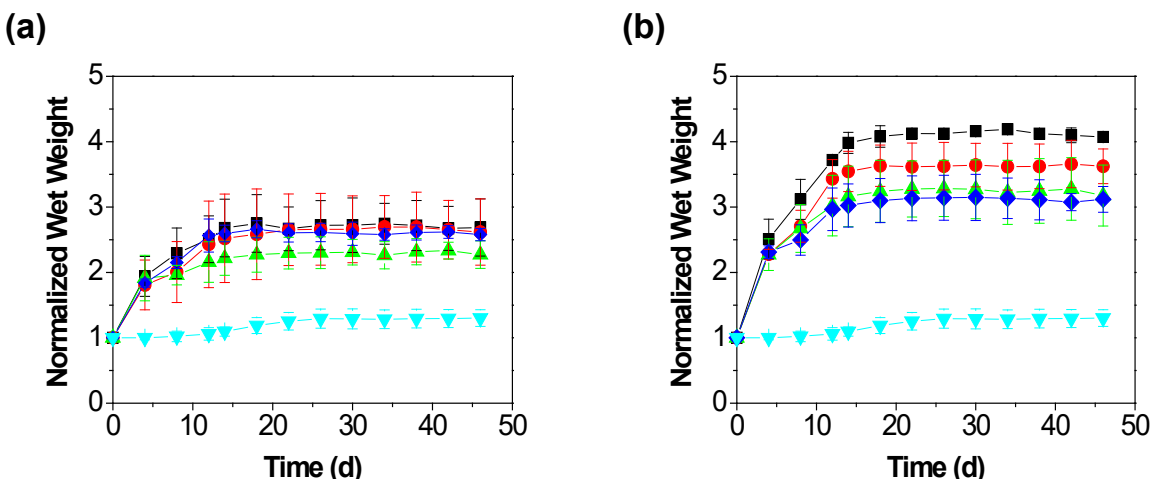


Figure 3. Effect of TW:TC ratio on coacervate swelling in tap water where (a) 32 mM TC and (b) 160 mM TC were initially added to the parent PAH solutions in (◆) 0.25:1, (▲) 0.33:1, (●) 0.50:1 and (■) 1.00:1 TW:TC molar ratios. For comparison, the swelling of control coacervates (▼) without any TC or TW is also shown. All data are mean \pm SD, while the solid curves are guides to the eye.

The moderate increase in swelling of the payload-free coacervates when placed in water was consistent with those previously reported for both PAH/TPP networks^{42, 45} and polyelectrolyte complex coacervates (prepared through the mixing of oppositely charged polymers).^{52, 53} Moreover, the increase in swelling with the coacervate loading was qualitatively similar to that seen in prior work upon the encapsulation of a non-binding zwitterionic dye (Rhodamine B).⁴² Because the LCs with the dye molecules were orders of magnitude lower than those used here, however, the swelling in that earlier work was much more modest (with the coacervate weights changing by just 10 – 30% when placed in deionized water or phosphate-buffered saline).⁴² Interestingly, in another prior study where PAH/TPP coacervates were loaded with the weakly amphiphilic, anionic drug, ibuprofen (whose LCs reached ~300 mg/g), the swelling was also very low, with 20 – 30% coacervate weight changes.⁴⁵ In the present case of TC/TW mixtures, however, the high solute content was combined with the introduction of network-disrupting insoluble TC particles, which (together with the TW micelles) may have impacted the swelling. Though the reasons for the much higher swelling of TC-loaded coacervates are not fully understood, it clearly illustrates that PAH/TPP coacervate swelling can be highly sensitive to their cargo content. Nonetheless, despite their moderate deformation upon swelling, the coacervates — like in prior reports^{42, 45} — remained intact throughout all multi-month swelling and release experiments (see Section 3.4) and maintained their adhesion to the agitated microcentrifuge tubes. Thus, the PAH/TPP coacervates (at least in the experimental setup used here) remained at their application sites over highly extended times.

3.4. TC Release Kinetics

Release over multi-month timescales was achieved using all tested coacervate compositions, with no more than ~ 50% of the TC released over 48 d (Figure 4). Yet, both the

release rate and release profile shape depended on the TC and TW concentrations used during coacervate preparation. Higher TC concentrations and TW:TC ratios generally produced faster release, with the TC release over the 48-d initial experiment increasing from roughly 1.1 to 5.7 mg (Figure 4a, c and e). At low TC loadings and TW:TC ratios, the release rates were relatively constant. At higher TC loadings and TW:TC concentrations (e.g., coacervates prepared by dispersing 160 mM TC in the parent PAH solution at 0.50:1 and 1.00:1 TW:TC molar ratio), however, there was a significant burst release. When the initial TC content was low (such as where 32 mM TC was dispersed in the parent PAH solution) and the TW:TC molar ratio was high (0.50 and 1.00:1), this burst release lasted only 2 d, after which slower release continued at a fairly constant rate (Figure 4a and b). When higher TC contents were used, however, the burst release at the same TW:TC ratios tended to persist for over a week (Figure 4e and f). This longer burst release period was followed by a relatively slow release rate during the second and third week, whereupon, after the third week, the release rate increased once again (Figure 4c – f). Interestingly, the burst release period also coincided with turbidity in the release media, which increased with both the TC content and TW:TC molar ratio, and suggested that the burst release (at least in part) stemmed from the ejection of colloidal TC particles from the coacervates. The accelerated release after the third week, on the other hand, may have reflected the coacervate becoming more swollen (Figure 3b) and, thus, more permeable to the encapsulated solutes (both TC and the solubility-enhancing TW). Further, the general increase in the release rate with the TW content likely stemmed from its impact on the TC solubility, in both the coacervate matrix and (because of the TW leaching into the tap water) the release medium. This TW leaching (i.e., the release of TW along with the TC) was evident from the foaming of the release media upon its agitation, which confirmed the surfactant release.

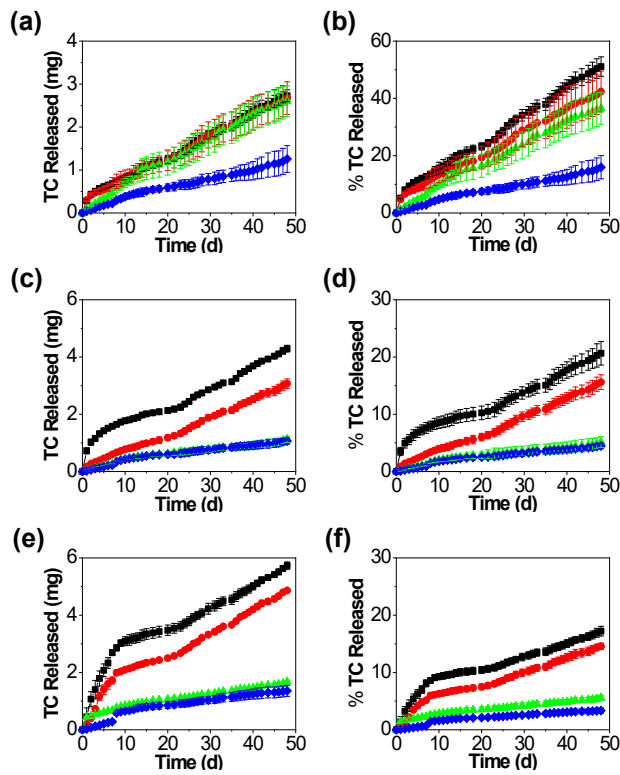


Figure 4. TC release from coacervates prepared by dispersing (a, b) 32 mM, (c, d) 97 mM and (e, f) 160 mM TC in the parent PAH solutions, where (\blacklozenge) 0.25:1, (\blacktriangle) 0.33:1, (\bullet) 0.50:1 and (\blacksquare) 1.00:1 TW:TC molar ratios were used. The release profiles are shown in terms of both (a, c, e) total TC mass released and (b, d, f) percent of encapsulated TC released as functions of time. All data are mean \pm SD.

Due to the hydrophobicity/low solubility of TC, its release profiles also depended on the choice of release medium volumes. At a low TW:TC molar ratio (of 0.25:1), where there was no burst release, the initial release rate became severalfold faster (roughly fivefold initially) when the release medium volume was raised tenfold (see Figure 5a, c and e). This difference suggested that sink conditions were not achieved and that the release rate was limited by the TC accumulation in the release media (which reduced the thermodynamic driving force for further TC release by, at least partially, saturating the release media). Over time, however, the release rate into the higher tap water volume slowed down and the effect of release medium volume diminished. This slowing of the release likely reflected a larger diffusion barrier at longer release times, at which the TC

near the surface of the coacervate was already released. Indeed, after approximately one month, the release rate became independent of the release medium volume, suggesting that — though they were not reliably accessed during initial timepoints — sink conditions during these long-term release experiments were eventually achieved.

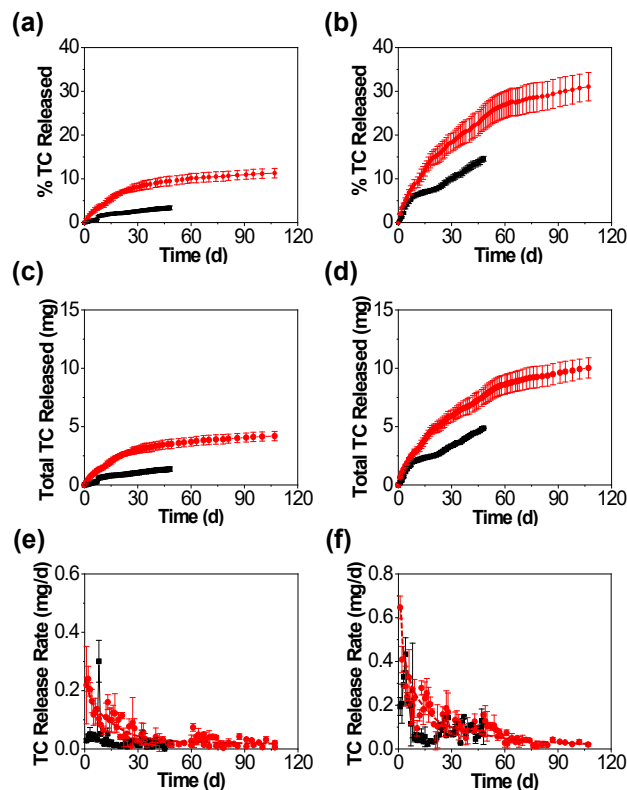


Figure 5. TC release from coacervates prepared by dispersing 160 mM TC in the parent PAH solution shown in terms of (a, b) percent of encapsulated TC released, (c, d) total TC mass released and (e, f) TC release rate as functions of time. The release profiles were obtained using (a, c, e) 0.25:1 and (b, d, f) 0.50:1 TW:TC molar ratios and either (■) 1 mL or (●) 10 mL of pH > 9.5 tap water as the release media. All data are mean \pm SD, while the dashed red curves are guides to the eye.

Also interesting was the effect of release medium volume at the higher, 0.50:1 TW:TC molar ratio, where a significant burst release occurred over the first week (Figure 5b, d and f). During the roughly week-long burst release period seen with the lower release medium volume — during which (regardless of the release medium volume) the release medium was turbid — the

release profiles obtained with the two dissimilar release medium volumes essentially overlapped (Figure 5b, d and f). This overlap likely reflected the TC being primarily released as colloidal particles rather than as dissolved molecules, which meant that it was not hindered by the saturation effects at lower release medium volumes. After this initial period, however, the release profiles began to diverge. While the release rate obtained using the lower water volume dropped sharply, the average release rate into the higher water volume exhibited only a very gradual reduction. Thus, upon the transition from the release of particulate TC to the release of solubilized TC, saturation/solute partitioning effects became significant, and the average release rate into 10 mL of tap water became roughly 5 – 6 fold higher than that into 1 mL of tap water. Finally, after about 3 weeks, at which point the release rate into the lower tap water volume sped up again, the release rates into the two release medium volumes again became similar, once more suggesting sink conditions to have been achieved at longer release times.

Overall, as the release medium volume was increased, the biphasic release profile shape was lost, and the release profiles become more monotonic (red circles in Figure 5b and d). Regardless of the TW:TC molar ratio and daily fluctuations in the measured release rates, release under these conditions generally slowed down with time as shown by the dashed lines in Figure 5e and f. Moreover, despite the increased release medium volume, highly sustained release of TC from the PAH/TPP coacervates was still achieved, with only roughly 10 – 35% of the payload released over 110 d. These release profiles show that, just like with water-soluble payloads studied previously,^{42, 45} PAH/TPP coacervates can enable long-term sustained release of hydrophobic payloads (including bactericides such as TC).

3.5. Antimicrobial Efficacy

The sustained TC release produced significant antibacterial activity against both model gram-positive (*S. aureus*) and model gram-negative (*E. coli*) bacteria over multiple weeks. Their fluorescence imaging in the presence of propidium iodide and thiazole orange stains revealed that, while in the absence of coacervates the cells were mostly viable, cells incubated in the presence of TC-eluting coacervates were — at least over the first two weeks — predominantly either damaged or dead (see Figures 6, 7a and 7b). For both *E. coli* and *S. aureus*, TC-loaded coacervates (with the exception of one data point) produced a 90 – 100% reduction in average cell viability over the first 15 d of the experiment (see Figure 7a and b). After 30 d of releasing TC, there was still significant antibacterial activity ($p < 0.05$), with only roughly half of the cells remaining viable. This activity, however, was substantially weaker than that earlier in the release process and, at the time points beyond one month (i.e., at 45 and 60 d into the release process), the antibacterial activity appeared to be fully lost (Figures 6, 7a, 7b and Supporting Information, Figure S2).

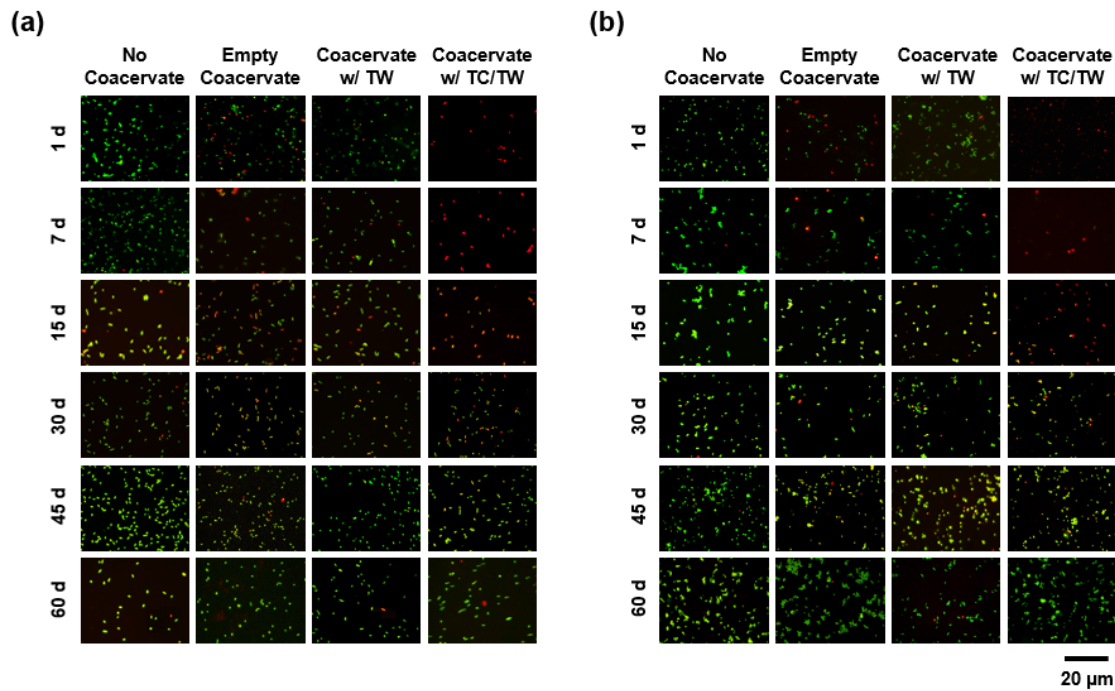


Figure 6. Representative fluorescence micrographs showing the viability of (a) *E. coli* and (b) *S. aureus* cells cultured in the presence of antibacterial PAH/TPP coacervates overnight (in 1/10× LB medium at 37 °C). Bacterial viability was detected using propidium iodide and thiazole orange stains at different time points in the release process. The leftmost column shows coacervate-free (control) growth condition, while the second, third and fourth columns show cell growth in the presence of empty coacervate, coacervate loaded with TW (but not TC), and TC/TW-loaded, biocide-eluting coacervate (prepared by dispersing 160 mM TC in the parent PAH solution at the 0.50:1 TW:TC molar ratio). Nonviable bacteria appear red, viable bacteria appear green, and damaged/membrane-compromised cells appear either yellow or orange.

Additionally, even without any TC or TW, the control coacervate was mildly antibacterial and (at least during some of the earlier time points) decreased the mean viability of both bacterial strains by 20 – 40% (with $p < 0.05$ at day 1 for *E. coli* and days 1 and 15 for *S. aureus*; Figures 6, 7a and 7b). This antibacterial activity may have been due to the bactericidal properties of PAH, which have previously been reported in studies on PAH hydrogels,⁵⁴ polyelectrolyte complex multilayer films,⁵⁵ and covalently modified surfaces.⁵⁶ Yet, this antibacterial activity tended to be mild relative to that of their TC-bearing counterparts

and, interestingly, was reduced by the addition of TW into the coacervates (in the presence of which the TC-free coacervates produced no significant bactericidal activity; see Figures 6, 7a, 7b and Supporting Information, Figure S2). This TW-mediated reduction in antibacterial activity was possibly due to a shielding of the cationic PAH by the surfactant and (consistent with prior findings)⁵⁷ suggested that TW was nontoxic to the bacteria.

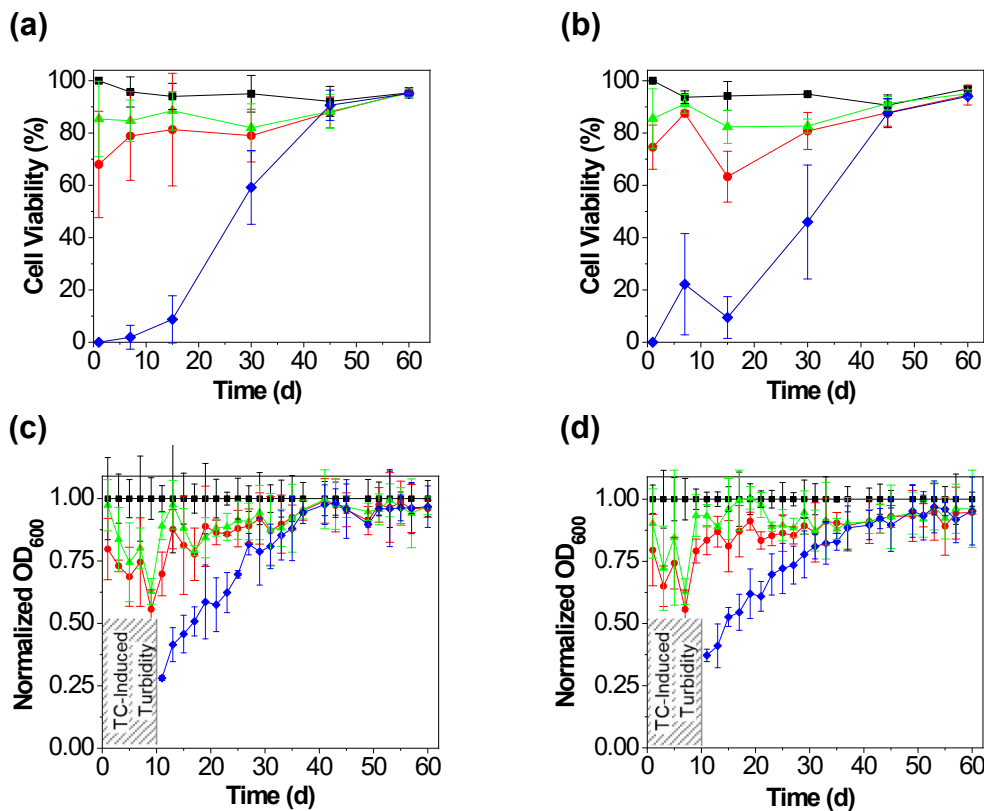


Figure 7. Analysis of (a, b) cell viability and (c, d) normalized optical density (to the coacervate-free control) over time upon culturing (a, c) *E. coli* and (b, d) *S. aureus* cells (■) under coacervate-free (control) growth conditions and in the presence of (●) empty coacervate, (▲) TW-loaded coacervate and (◆) TC/TW-loaded coacervate. The TC-eluting coacervate was formulated by dispersing 160 mM TC in the parent PAH solution at the 0.50:1 TW:TC molar ratio and all planktonic cultures were grown in 1/10 \times LB medium at 37 °C. All data are mean \pm SD, while the lines are guides to the eye.

The above microscopy observations were also supported by OD measurements, which revealed the relative numbers of cells (either live or dead) present upon exposure to each condition

(Figure 7c and d). Due to the turbidity caused by the release of colloidal TC particles during the early time points (see Section 3.4), OD data reflecting cell growth could not be reliably collected from cultures exposed to TC-eluting coacervates during the first ~10 d of the release process. Nonetheless, it was clear that: (1) the cell numbers were lowest for the TC-eluting coacervates, with a significant ($p < 0.05$) antibacterial effect against *E. coli* and *S. aureus* occurring for the first 33 and 35 d, respectively; (2) even TC-free coacervates had an antibacterial (or at least an inhibitory) effect, though this effect was only occasionally significant; and (3) that the antibacterial effect diminished with time and, after about 1 month, disappeared. Further, the normalized cell numbers revealed by the OD measurements — which, after 15 and 30 d, were in the 40 – 50% and roughly 80% range, respectively — were much higher than the percentages of viable cells at those time points. Since the OD measurements did not distinguish between viable and nonviable cells, however, these quantitative differences between OD and cell viability results were both expected and consistent with those seen in other antibacterial activity studies.^{58, 59}

Collectively, the fluorescence microscopy and OD measurements indicated that, despite the multi-month TC release obtained using the PAH/TPP coacervates, the antibacterial activity (where $p < 0.05$) was limited to only a few weeks. This shorter duration of their effectiveness likely reflected the gradual reduction in the average TC release rate with time. Indeed, according to the curve drawn through the release data for the coacervate formulation used in the antibacterial activity experiment (see dashed red curve in Figure 5f), the average TC release rate decreased from above 0.6 to below ~ 0.1 mg/d in the first month of the release profile, thereby reducing the TC concentration accumulated in the release media after 1 d from 60 – 70 to roughly 10 mg/L. Thus, the gradual reduction in the release rates over the first month dropped the accumulated TC concentrations from being significantly above the reported minimum bactericidal concentrations

(MBC), which were 4 mg/L for *E. coli* (25922)⁵⁸ and 1 mg/L for *S. aureus* (25923),⁶⁰ to being within an order of magnitude as those MBCs. Although the literature values were obtained under different test conditions (which could explain the quantitative difference in TC requirements), their ballpark comparison with the released TC concentrations supported the view that the TC release eventually became too slow. This eventual loss of biocidal activity was also qualitatively consistent with prior findings on TC release from slowly-releasing polystyrene films where, due to an even slower release, antibacterial activity was lost after the first few hours.⁶¹ Further, the decreased antibacterial activity due to PAH on the coacervate surface (which initially showed bactericidal effects even in the absence of TC; Figures 6 and 7) may have reflected biofilm formation on the surface of the coacervates (see Supporting Information, Section C) which, after repeated exposure to bacteria, reduced the availability of biocidal surface PAH chains.

Despite these observations and the bactericidal activity duration being shorter than the TC release profile, the bactericide-loaded PAH/TPP coacervates produced a highly sustained antibacterial effect (see Figures 6 and 7), which killed most of the bacteria for at least two weeks and was still discernable after one month. Also important was that, to minimize cell death in the absence of bactericidal treatment, these bactericidal properties were evaluated under conditions that were more favorable to bacterial survival than those present in most disinfection applications (i.e., the cells were cultured in 1/10× LB medium rather than regular tap water). Thus, the duration of the antibacterial effect measured in this study may have been lower than those expected in many of the potential coacervate applications, where (in the absence of growth media) bacterial survival would likely be diminished. To ascertain the true duration of their (application-specific) long-term bactericidal effect, further analyses of their antibacterial properties in various types of media-free water (and under varying flow conditions) should therefore be performed in future work.

3.6. Technological Implications

The multi-week antibacterial effect achieved with PAH/TPP coacervates could be utilized in diverse applications, where the coacervates may be attached to a wet surface/device and provide sustained disinfection. Although TC (and TW) encapsulation decreases the tackiness of the coacervate, TC-loaded PAH/TPP networks can still be adhered to surfaces (i.e., through either their own residual adhesiveness, or by attaching a tackier TC-free PAH/TPP coacervate layer, to serve as the adhesive). Further, since solute permeability of PAH/TPP coacervates can be increased (e.g., by partially disrupting PAH/TPP association through anionic surfactant inclusion),⁴⁵ it is likely that — by accelerating/optimizing the TC release from the coacervates (or, alternatively, choosing a different bactericide) — an even longer-term antibacterial effect might be achieved.

Overall, the PAH/TPP coacervates enable longer-term bactericide release and antibacterial activity than those generally reported for hydrogels (which, like the coacervates, are aqueous polymer networks, but tend to have more hydrated/permeable network structures).⁴² Despite multi-week bactericide (silver ion) release having been achieved by loading the gels with slowly dissolving silver nanoparticles,^{28, 31} hydrogels tend to (due to their higher permeability) release most of their small-molecule cargos within one day²⁹⁻³¹ and are typically only demonstrated to be antibacterial over short observation times, ranging from hours²⁹⁻³¹ to a couple of days.^{14, 28} Conversely, the present study shows that bactericide-eluting PAH/TPP coacervates can kill most of the bacteria for at least two weeks, with a statistically significant antibacterial effect (albeit a weakened one) persisting after a month.

Though there have been reports of antimicrobial-releasing PEM films providing fungicidal and bacterial colonization-disrupting activity over even longer timescales than shown here,^{40, 41}

the PAH/TPP polyelectrolyte-based biocide release systems benefit from much simpler/quicker preparation procedures (both of which could ultimately facilitate their use in commercial applications). Moreover, unlike the PEM films, the putty-like coacervates can be more easily molded (i.e., customized after their initial preparation) to their manifold potential application sites and, once they lose their efficacy, removed and reapplied.

Another category of materials that has been occasionally reported to provide a longer-term antibacterial activity than that shown herein are certain types of plastic films and polymer elastomers, which enable release/antibacterial activity over a multi-month timescale.^{16, 19} Nonetheless, since the PAH/TPP coacervates form under milder conditions (e.g., without high-temperature processing or synthetic chemical reactions), they may offer attractive alternatives to these plastic-based disinfection technologies.

We envision that these PAH/TPP coacervate-based bactericide or fungicide releasing devices could be attractive for diverse household, dental and hospital applications, to prevent the growth of harmful microbes on wet surfaces. These potential applications include sustained disinfection of household and hospital shower heads and hoses,⁶²⁻⁶⁴ dental unit waterlines,^{65, 66} sink drains,^{67, 68} washing machines,⁶⁹ sponges and dish/wash cloths,⁶⁷ and even bath toys (or other items that remains wet between uses).⁴ Another potential class of bactericide-eluting PAH/TPP coacervate uses could be in disinfecting building and automotive heating, ventilation and air conditioning (HVAC) system components, where bacterial growth can lead to both infections and foul odors.⁷⁰ Finally, though these applications remain to be experimentally explored, these coacervates may find use as infection-preventing parts of non-degradable surgical implants and indwelling catheters.

4. CONCLUSIONS

We have shown that PAH/TPP coacervates can efficiently encapsulate high loadings of hydrophobic bactericides and release them over multiple-month timescales. The encapsulation process is facilitated through the addition of nonionic surfactant, and the LC within these resulting coacervates can be predictably tuned by varying the amount of added bactericide. The bactericide release rate is also readily adjusted by varying its loading and the surfactant:bactericide ratio used in the coacervate preparation and, when room-temperature tap water is used as the release medium, enables sustained release over more than 3 months. This sustained release imparts PAH/TPP coacervates — which, even without bactericide, exhibit mild antibacterial activity — with significant antibacterial activity over several weeks (i.e., over an extended period, albeit one shorter than the full duration of their release profile). The bactericidal effect (even in the nutrient-rich environment used in this work) kills most of the bacteria over two weeks and roughly half of the bacteria after one month. At longer times, however, the bactericide release becomes too slow to be efficacious, and the antibacterial activity is fully lost. Collectively, these findings support the possibility of using bactericide-eluting PAH/TPP coacervates for controlling microbial growth in diverse applications, such as household, hospital and dental office disinfection, or medical device design.

ASSOCIATED CONTENT

Supporting Information. Photographs showing variations in supernatant turbidity upon TC encapsulation; statistical analysis of antibacterial analysis data showing the conditions/time points with statistically significant bactericidal activity; crystal violet staining revealing eventual biofilm

formation on the TC-free coacervate surfaces. This material is available free of charge via the Internet at <http://pubs.acs.org>.

AUTHOR INFORMATION

Corresponding Authors

* Email: yakov.lapitsky@utoledo.edu (Y.L.); Email: youngwoo.seo@utoledo.edu (Y.S.).

Author Contributions

The manuscript was written through contributions of all authors. All authors have given approval to the final version of the manuscript.

ACKNOWLEDGMENT

The authors gratefully acknowledge the National Science Foundation (IIP-1701104) for the financial support of this work, and Univ. of Toledo's Kunal Choudhuri (UV-vis spectroscopy), Lei Li (fluorescence microscopy), and Anusha Kadudula and Parul Baranwal (microbiology lab techniques) for experimental assistance.

REFERENCES

1. Cabral, J. P., Water microbiology. Bacterial pathogens and water. *Int. J. Environ. Res. Public Health* **2010**, *7* (10), 3657-3703.
2. Kolter, R.; Greenberg, E. P., The superficial life of microbes. *Nature* **2006**, *441* (7091), 300-302.
3. Galie, S.; García-Gutiérrez, C.; Miguélez, E. M.; Villar, C. J.; Lombó, F., Biofilms in the food industry: health aspects and control methods. *Front. Microbiol.* **2018**, *9*, 898.
4. Neu, L.; Bänziger, C.; Proctor, C. R.; Zhang, Y.; Liu, W.-T.; Hammes, F., Ugly ducklings—the dark side of plastic materials in contact with potable water. *NPJ Biofilms Microbiomes* **2018**, *4* (1), 7.

5. Hong, C.; Moorman, G., Plant pathogens in irrigation water: challenges and opportunities. *Crit. Rev. Plant Sci.* **2005**, *24* (3), 189-208.
6. Mansfield, J.; Genin, S.; Magori, S.; Citovsky, V.; Sriariyanum, M.; Ronald, P.; Dow, M.; Verdier, V.; Beer, S. V.; Machado, M. A., Top 10 plant pathogenic bacteria in molecular plant pathology. *Mol. Plant Pathol.* **2012**, *13* (6), 614-629.
7. Flemming, H., Biofouling and me: My Stockholm syndrome with biofilms. *Water Res.* **2020**, *115576*.
8. Batmanghelich, F.; Li, L.; Seo, Y., Influence of multispecies biofilms of *Pseudomonas aeruginosa* and *Desulfovibrio vulgaris* on the corrosion of cast iron. *Corros. Sci.* **2017**, *121*, 94-104.
9. Mori, T.; Nonaka, T.; Tazaki, K.; Koga, M.; Hikosaka, Y.; Noda, S., Interactions of nutrients, moisture and pH on microbial corrosion of concrete sewer pipes. *Water Res.* **1992**, *26* (1), 29-37.
10. Karsa, D. R.; Ashworth, D., *Industrial biocides: selection and application*. R. Soc. Chem.: 2007.
11. Maillard, J.-Y., Antimicrobial biocides in the healthcare environment: efficacy, usage, policies, and perceived problems. *Ther. Clin. Risk Manag.* **2005**, *1* (4), 307.
12. Sofokleous, P.; Ali, S.; Wilson, P.; Buanz, A.; Gaisford, S.; Mistry, D.; Fellows, A.; Day, R. M., Sustained antimicrobial activity and reduced toxicity of oxidative biocides through biodegradable microparticles. *Acta Biomater.* **2017**, *64*, 301-312.
13. Trojer, M. A.; Nordstierna, L.; Bergek, J.; Blanck, H.; Holmberg, K.; Nyden, M., Use of microcapsules as controlled release devices for coatings. *Adv. Colloid Interface Sci.* **2015**, *222*, 18-43.
14. Hu, Y.; Ren, G.; Deng, L.; Zhang, J.; Liu, H.; Mu, S.; Wu, T., Degradable UV-crosslinked hydrogel for the controlled release of triclosan with reduced cytotoxicity. *Mater. Sci. Eng. C* **2016**, *67*, 151-158.
15. Manna, U.; Raman, N.; Welsh, M. A.; Zayas-Gonzalez, Y. M.; Blackwell, H. E.; Palecek, S. P.; Lynn, D. M., Slippery Liquid-Infused Porous Surfaces that Prevent Microbial Surface Fouling and Kill Non-Adherent Pathogens in Surrounding Media: A Controlled Release Approach. *Adv. Funct. Mater.* **2016**, *26* (21), 3599-3611.
16. McBride, M. C.; Malcolm, R. K.; Woolfson, A. D.; Gorman, S. P., Persistence of antimicrobial activity through sustained release of triclosan from pegylated silicone elastomers. *Biomaterials* **2009**, *30* (35), 6739-6747.
17. Ruggeri, V.; Francolini, I.; Donelli, G.; Piozzi, A., Synthesis, characterization, and in vitro activity of antibiotic releasing polyurethanes to prevent bacterial resistance. *J. Biomed. Mater. Res., Part A* **2007**, *81* (2), 287-298.
18. Mattos, B. D.; Tardy, B. L.; Pezhman, M.; Kämäräinen, T.; Linder, M.; Schreiner, W. H.; Magalhães, W. L.; Rojas, O. J., Controlled biocide release from hierarchically-structured biogenic silica: surface chemistry to tune release rate and responsiveness. *Sci. Rep.* **2018**, *8* (1), 1-11.

19. Iconomopoulou, S.; Voyatzis, G., The effect of the molecular orientation on the release of antimicrobial substances from uniaxially drawn polymer matrixes. *J. Controlled Release* **2005**, *103* (2), 451-464.
20. Bromberg, L. E.; Braman, V. M.; Rothstein, D. M.; Spacciapoli, P.; O'Connor, S. M.; Nelson, E. J.; Buxton, D. K.; Tonetti, M. S.; Friden, P. M., Sustained release of silver from periodontal wafers for treatment of periodontitis. *J. Controlled Release* **2000**, *68* (1), 63-72.
21. Bromberg, L. E.; Buxton, D. K.; Friden, P. M., Novel periodontal drug delivery system for treatment of periodontitis. *J. Controlled Release* **2001**, *71* (3), 251-259.
22. Nori, M. P.; Fávaro-Trindade, C. S.; de Alencar, S. M.; Thomazini, M.; de Carvalho Balieiro, J. C.; Contreras Castillo, C. J., Microencapsulation of propolis extract by complex coacervation. *LWT-Food Sci. Technol.* **2011**, *44*, 429-435.
23. Suarez, S.; O'Hara, P.; Kazantseva, M.; Newcomer, C. E.; Hopfer, R.; McMurray, D. N.; Hickey, A. J., Respirable PLGA microspheres containing rifampicin for the treatment of tuberculosis: screening in an infectious disease model. *Pharm. Res.* **2001**, *18* (9), 1315-1319.
24. Chen, Z.; Luo, J.; Sun, Y., Biocidal efficacy, biofilm-controlling function, and controlled release effect of chloromelamine-based bioresponsive fibrous materials. *Biomaterials* **2007**, *28* (9), 1597-1609.
25. Torres-Giner, S.; Lagaron, J. M., Zein-based ultrathin fibers containing ceramic nanofillers obtained by electrospinning. I. Morphology and thermal properties. *J. Appl. Polym. Sci.* **2010**, *118* (2), 778-789.
26. Böttcher, H.; Jagota, C.; Trepte, J.; Kallies, K.-H.; Haufe, H., Sol-gel composite films with controlled release of biocides. *J. Controlled Release* **1999**, *60* (1), 57-65.
27. Popat, K. C.; Eltgroth, M.; LaTempa, T. J.; Grimes, C. A.; Desai, T. A., Decreased *Staphylococcus epidermidis* adhesion and increased osteoblast functionality on antibiotic-loaded titania nanotubes. *Biomaterials* **2007**, *28* (32), 4880-4888.
28. Fullenkamp, D. E.; Rivera, J. G.; Gong, Y.-k.; Lau, K. A.; He, L.; Varshney, R.; Messersmith, P. B., Mussel-inspired silver-releasing antibacterial hydrogels. *Biomaterials* **2012**, *33* (15), 3783-3791.
29. Hoque, J.; Haldar, J., Direct synthesis of dextran-based antibacterial hydrogels for extended release of biocides and eradication of topical biofilms. *ACS Appl. Mater. Interfaces* **2017**, *9* (19), 15975-15985.
30. Johnson, C. T.; Wroe, J. A.; Agarwal, R.; Martin, K. E.; Guldberg, R. E.; Donlan, R. M.; Westblade, L. F.; García, A. J., Hydrogel delivery of lysostaphin eliminates orthopedic implant infection by *Staphylococcus aureus* and supports fracture healing. *Proc. Natl. Acad. Sci.* **2018**, *115* (22), E4960-E4969.
31. Rattanaruengsrikul, V.; Pimpha, N.; Supaphol, P., Development of gelatin hydrogel pads as antibacterial wound dressings. *Macromol. Biosci.* **2009**, *9* (10), 1004-1015.
32. Grunlan, J. C.; Choi, J. K.; Lin, A., Antimicrobial behavior of polyelectrolyte multilayer films containing cetrimide and silver. *Biomacromolecules* **2005**, *6* (2), 1149-1153.

33. Li, Z.; Lee, D.; Sheng, X.; Cohen, R. E.; Rubner, M. F., Two-level antibacterial coating with both release-killing and contact-killing capabilities. *Langmuir* **2006**, *22* (24), 9820-9823.

34. Pavlukhina, S.; Lu, Y.; Patimetha, A.; Libera, M.; Sukhishvili, S., Polymer multilayers with pH-triggered release of antibacterial agents. *Biomacromolecules* **2010**, *11* (12), 3448-3456.

35. Deka, C.; Deka, D.; Bora, M. M.; Jha, D. K.; Kakati, D. K., Synthesis of peppermint oil-loaded chitosan/alginate polyelectrolyte complexes and study of their antibacterial activity. *J. Drug Deliv. Sci. Tech.* **2016**, *35*, 314-322.

36. Yu, S. H.; Mi, F. L.; Wu, Y. B.; Peng, C. K.; Shyu, S. S.; Huang, R. N., Antibacterial activity of chitosan–alginate sponges incorporating silver sulfadiazine: Effect of ladder-loop transition of interpolyelectrolyte complex and ionic crosslinking on the antibiotic release. *J. Appl. Polym. Sci.* **2005**, *98* (2), 538-549.

37. Shahgholian, N.; Rajabzadeh, G., Fabrication and characterization of curcumin-loaded albumin/gum arabic coacervate. *Food Hydrocoll.* **2016**, *59*, 17-25.

38. Kyffin, B. A.; Foroutan, F.; Raja, F. N.; Martin, R. A.; Pickup, D. M.; Taylor, S. E.; Carta, D., Antibacterial silver-doped phosphate-based glasses prepared by coacervation. *J. Mater. Chem. B* **2019**, *7* (48), 7744-7755.

39. Pickup, D. M.; Newport, R. J.; Barney, E. R.; Kim, J.-Y.; Valappil, S. P.; Knowles, J. C., Characterisation of phosphate coacervates for potential biomedical applications. *J. Biomater. Appl.* **2014**, *28* (8), 1226-1234.

40. Kratochvil, M. J.; Tal-Gan, Y.; Yang, T.; Blackwell, H. E.; Lynn, D. M., Nanoporous superhydrophobic coatings that promote the extended release of water-labile quorum sensing inhibitors and enable long-term modulation of quorum sensing in *Staphylococcus aureus*. *ACS Biomater. Sci. Eng.* **2015**, *1* (10), 1039-1049.

41. Raman, N.; Lee, M.-R.; Palecek, S. P.; Lynn, D. M., Polymer multilayers loaded with antifungal β -peptides kill planktonic *Candida albicans* and reduce formation of fungal biofilms on the surfaces of flexible catheter tubes. *J. Controlled Release* **2014**, *191*, 54-62.

42. Lawrence, P. G.; Patil, P. S.; Leipzig, N. D.; Lapitsky, Y., Ionically cross-linked polymer networks for the multiple-month release of small molecules. *ACS Appl. Mater. Interfaces* **2016**, *8* (7), 4323-4335.

43. Huang, Y.; Lawrence, P. G.; Lapitsky, Y., Self-assembly of stiff, adhesive and self-healing gels from common polyelectrolytes. *Langmuir* **2014**, *30* (26), 7771-7777.

44. Lawrence, P. G.; Lapitsky, Y., Ionically cross-linked poly(allylamine) as a stimulus-responsive underwater adhesive: ionic strength and pH effects. *Langmuir* **2015**, *31* (4), 1564-1574.

45. de Silva, U. K.; Brown, J. L.; Lapitsky, Y., Poly(allylamine)/tripolyphosphate coacervates enable high loading and multiple-month release of weakly amphiphilic anionic drugs: an in vitro study with ibuprofen. *RSC Adv.* **2018**, *8* (35), 19409-19419.

46. Goldsmith, D. R.; Scott, L. J.; Cvetković, R. S.; Plosker, G. L., Sevelamer hydrochloride. *Drugs* **2008**, *68* (1), 85-104.

47. Jones, R. D.; Jampani, H. B.; Newman, J. L.; Lee, A. S., Triclosan: a review of effectiveness and safety in health care settings. *Am. J. Infect. Control* **2000**, *28* (2), 184-196.
48. Russell, A., Whither triclosan? *J. Antimicrob. Chemother.* **2004**, *53* (5), 693-695.
49. Leclercq, S.; Harlander, K. R.; Reineccius, G. A., Formation and characterization of microcapsules by complex coacervation with liquid or solid aroma cores. *Flavour Frag. J.* **2009**, *24* (1), 17-24.
50. Yang, X.; Gao, N.; Hu, L.; Li, J.; Sun, Y., Development and evaluation of novel microcapsules containing poppy-seed oil using complex coacervation. *J. Food Eng.* **2015**, *161*, 87-93.
51. Kastellorizios, M.; Burgess, D. J., In vitro drug release testing and in vivo/in vitro correlation for long acting implants and injections. In *Long Acting Injections and Implants*, Springer: 2012; pp 475-503.
52. Fares, H. M.; Wang, Q.; Yang, M.; Schlenoff, J. B., Swelling and inflation in polyelectrolyte complexes. *Macromolecules* **2018**, *52* (2), 610-619.
53. Hamad, F. G.; Chen, Q.; Colby, R. H., Linear viscoelasticity and swelling of polyelectrolyte complex coacervates. *Macromolecules* **2018**, *51* (15), 5547-5555.
54. Andrews, M. A.; Figuly, G. D.; Chapman, J. S.; Hunt, T. W.; Glunt, C. D.; Rivenbark, J. A.; Chenault, H. K., Antimicrobial hydrogels formed by crosslinking polyallylamine with aldaric acid derivatives. *J. Appl. Polym. Sci.* **2011**, *119* (6), 3244-3252.
55. Licher, J. A.; Rubner, M. F., Polyelectrolyte multilayers with intrinsic antimicrobial functionality: the importance of mobile polycations. *Langmuir* **2009**, *25* (13), 7686-7694.
56. Iarikov, D. D.; Kargar, M.; Sahari, A.; Russel, L.; Gause, K. T.; Behkam, B.; Ducker, W. A., Antimicrobial surfaces using covalently bound polyallylamine. *Biomacromolecules* **2013**, *15* (1), 169-176.
57. Bartůněk, V.; Junková, J.; Šuman, J.; Kolářová, K.; Rimpelová, S.; Ulbrich, P.; Sofer, Z., Preparation of amorphous antimicrobial selenium nanoparticles stabilized by odor suppressing surfactant polysorbate 20. *Mater. Lett.* **2015**, *152*, 207-209.
58. Ellison, M. L.; Champlin, F. R., Outer membrane permeability for nonpolar antimicrobial agents underlies extreme susceptibility of *Pasteurella multocida* to the hydrophobic biocide triclosan. *Vet. Microbiol.* **2007**, *124* (3-4), 310-318.
59. Sondi, I.; Salopek-Sondi, B., Silver nanoparticles as antimicrobial agent: a case study on *E. coli* as a model for Gram-negative bacteria. *J. Colloid Interface Sci.* **2004**, *275* (1), 177-182.
60. Grandgirard, D.; Furi, L.; Ciusa, M. L.; Baldassarri, L.; Knight, D. R.; Morrissey, I.; Largiadèr, C. R.; Leib, S. L.; Oggioni, M. R., Mutations upstream of fabI in triclosan resistant *Staphylococcus aureus* strains are associated with elevated fabI gene expression. *BMC Genomics* **2015**, *16* (1), 345.
61. Kalyon, B. D.; Olgun, U., Antibacterial efficacy of triclosan-incorporated polymers. *Am. J. Infect. Control* **2001**, *29* (2), 124-125.

62. Feazel, L. M.; Baumgartner, L. K.; Peterson, K. L.; Frank, D. N.; Harris, J. K.; Pace, N. R., Opportunistic pathogens enriched in showerhead biofilms. *Proc. Natl. Acad. Sci.* **2009**, *106* (38), 16393-16399.
63. Moat, J.; Rizoulis, A.; Fox, G.; Upton, M., Domestic shower hose biofilms contain fungal species capable of causing opportunistic infection. *J. Water Health* **2016**, *14* (5), 727-737.
64. Soto-Giron, M. J.; Rodriguez-R, L. M.; Luo, C.; Elk, M.; Ryu, H.; Hoelle, J.; Santo Domingo, J. W.; Konstantinidis, K. T., Biofilms on hospital shower hoses: characterization and implications for nosocomial infections. *Appl. Environ. Microbiol.* **2016**, *82* (9), 2872-2883.
65. Ricci, M. L.; Fontana, S.; Pinci, F.; Fiumana, E.; Pedna, M. F.; Farolfi, P.; Sabattini, M. A. B.; Scaturro, M., Pneumonia associated with a dental unit waterline. *The Lancet* **2012**, *379* (9816), 684.
66. Ji, X. Y.; Fei, C. N.; Zhang, Y.; Liu, J.; Liu, H.; Song, J., Three key factors influencing the bacterial contamination of dental unit waterlines: a 6-year survey from 2012 to 2017. *International Dent. J.* **2019**, *69* (3), 192-199.
67. Hassan, K.; ElBagoury, M., The Domestic Kitchen—The ‘Front Line in the Battle Against Foodborne Disease’. *J. Pure App. Microbiol.* **2018**, *12* (1), 181-187.
68. McBain, A. J.; Bartolo, R. G.; Catrenich, C. E.; Charbonneau, D.; Ledder, R. G.; Rickard, A. H.; Symmons, S. A.; Gilbert, P., Microbial characterization of biofilms in domestic drains and the establishment of stable biofilm microcosms. *Appl. Environ. Microbiol.* **2003**, *69* (1), 177-185.
69. Jacksch, S.; Kaiser, D.; Weis, S.; Weide, M.; Ratering, S.; Schnell, S.; Egert, M., Influence of Sampling Site and other Environmental Factors on the Bacterial Community Composition of Domestic Washing Machines. *Microorganisms* **2020**, *8* (1), 30.
70. Schmidt, M. G.; Attaway, H. H.; Terzieva, S.; Marshall, A.; Steed, L. L.; Salzberg, D.; Hamoodi, H. A.; Khan, J. A.; Feigley, C. E.; Michels, H. T., Characterization and control of the microbial community affiliated with copper or aluminum heat exchangers of HVAC systems. *Curr. Microbiol.* **2012**, *65* (2), 141-149.

TOC Image

